Molecular Catalysis 493 (2020) 111104

Contents lists available at ScienceDirect

Molecular Catalysis

journal homepage: www.elsevier.com/locate/mcat

Metal silicotungstate salts as catalysts in furfural oxidation reactions with hydrogen peroxide

Márcio J. da Silva*, Alana A. Rodrigues

Chemistry Department, Federal University of Viçosa, Viçosa, 36570-000 MG, Brazil

ARTICLE INFO

Keywords:
Lewis acid metals
Keggin heteropoly salts
Furfural
Hydrogen peroxide

ABSTRACT

In this work, metal cations exchanged silicotungstic acid salts were synthesized and evaluated as catalysts in furfural oxidative esterification reactions with hydrogen peroxide in alkyl alcohols solution. The protons of silicotungstic acid were totally exchanged with Co^{2+}, Cu^{2+}, Ni^{2+}, Al^{3+}, and Fe^{3+} cations, generating catalysts that were characterized by infrared spectroscopy, X-rays diffraction patterns, energy dispersive spectroscopy, scan electronic microscopy images, and thermal analyses. Isotherms of adsorption/ desorption of nitrogen provided the surface area, distribution, volume, and pores diameter. The strength and amount of the acid sites were determined by potentiometric titration curves. Noticeably, the oxidation of furfural proceeded without opening the furan ring. Furoic acid and alkyl furoate were the main reaction products, with the formation of the furfural acetal as a secondary product. The effect of main reaction parameters such as the H_2O_2: furfural molar ratio, the catalyst amount, and the temperature were studied. The reactivity of the furfural with other alkyl alcohols was also assessed. The solid, active, and easily synthesizable catalyst, and the use of an inexpensive and environmentally benign oxidant are positive aspects of this selective process for oxidative esterification of furfural.

1. Introduction

Furfural has been produced from lignocellulose through chemical and thermal treatment [1,2]. Therefore, it is a useful potentially platform molecule in biorefinery processes to produce a plethora of renewable origin chemicals and biofuels [3]. Among the several routes to converting furfural to more value-added products, their oxidation in gas or liquid phase has attracted a lot attention [4,5]. Green oxidants such as molecular oxygen or hydrogen peroxide have been used due to environmental and economic reasons [6–8].

Industrially, furfural oxidation has been carried out via Cannizzaro reactions with NaOH, a homogenous process [9]. Alternatively, different processes to oxidize furfural have been developed, where ionic liquids, biphasic systems, organocatalysts, homogeneous or heterogeneous catalysts are present [10–14]. Molecular oxygen is an oxidant very used in reactions to converting furfural to derivatives using mainly supported solid transition metal as catalysts in superior alcohol solution [15,16]. Furfural has been also oxidized by molecular oxygen to maleic acid or anhydride, which are valuable compounds to fine chemical and pharmacy industries, over molybdenum and or vanadium solid catalysts [17,18]. However, besides being a flammable oxidant, high pressures of oxygen, temperatures, additives, and noble metal catalysts are sometimes required to perform the reactions [19–21].

On the other hand, hydrogen peroxide is an inexpensive oxidant and desirable in terms of atom economy, availability, and therefore it is particularly attractive and safe for industrial processes [22]. Nonetheless, it is always requiring the presence of a metal catalyst to activate the hydrogen peroxide. In this regard, titanium silicate demonstrated to be an efficient catalyst to convert furfural to maleic acid in oxidations with hydrogen peroxide in the aqueous phase [23,24]. However, a long reaction time (ca. > 24 h) was necessary to achieve high conversions and selectivity. Another strategy used is to perform the furfural oxidations in the presence of organic acids such as acetic acid, generating peracids which are the true terminal oxidants [25].

A lot of attention has been dedicated to developing oxidation processes of the furfural to their acyclic dicarboxylic acid derivatives over heterogeneous catalysts (i.e., succinic, and maleic acids), which are highly valuable chemicals [23,25,26]. Nonetheless, not always a high carbon efficiency has been achieved, mainly due to polymerization of the substrate. The use of co-catalysts in a biphasic system can reduce this effect [13].

On the other hand, alkyl furoates are derivatives blendable to the liquid fuels that can be produced through oxidative esterification of furfural with alkyl alcohols, in solid-catalyzed processes, such as

* Corresponding author at: Chemistry Department, Federal University of Viçosa, Avenida Peter Henry Rolfs, s/n, Viçosa, MG 36570-900, Brazil.
E-mail address: silvamj2003@ufv.br (M.J. da Silva).

https://doi.org/10.1016/j.mcat.2020.111104
Received 27 March 2020; Received in revised form 15 June 2020; Accepted 27 June 2020

supported Au nanoparticles [27,28]. Production at large scale of alkyl furoates starting from xyloses present in biomass residues may make these products attractive and economically viable for fine chemical industries [29]. In this regard, the oxidative esterification in one pot is an attractive alternative to the traditional processes that employ metal salts as stoichiometric oxidant and sulfuric acid as the catalyst [30].

Keggin heteropolyacids (HPAs) are a versatile class of metal-oxygen clusters active in acid-catalyzed or oxidations reactions [31,32]. Vanadium-Molybdenum heteropolyacids were successfully used as the catalysts in aerobic oxidations of 5-hydroxymethyl furfural to maleic acid and anhydride [33]. However, HPAs are soluble in a polar solvent, hampering their reuse. The conversion of HPAs to insoluble salts has been an approach that overcomes this drawback [34]. In addition, when the saturated heteropolyanion (i.e., $PW_{12}O_{40}^{3-}$, $SiW_{12}O_{40}^{4-}$) are converted to the lacunar anion (i.e., $PW_{11}O_{39}^{6-}$, $SiW_{11}O_{39}^{7-}$), these compounds become catalysts highly active in oxidations with hydrogen peroxide [35–39].

Another modification on the Keggin HPAs composition that has been successfully performed is their conversion to salts, where the acidic protons are partially or totally exchanged by metal cations [40]. This is an effective strategy mainly if the metal cation itself has demonstrated to be catalytically active; this is the case of Tin(II) cations, which were very active catalysts in esterification and etherification reactions [41–43]. Metal transition exchanged HPA salts were efficient catalysts in acetalization reactions of the glycerol with HOAc, mainly the $Fe_{4/3}SiW_{12}O_{40}$ salt [44]. Moreover, $Al_{4/3}SiW_{12}O_{40}$ salts were efficient catalysts in oxidation reactions of camphene with hydrogen peroxide [45].

In this work, we synthesized a series of metal silicotungstate salts (i.e., $M_{4/n}SiW_{12}O_{40}$; M^{n+} = Co^{2+}, Ni^{2+}, Cu^{2+}, Al^{3+}, and Fe^{3+}) and evaluating their catalytic activity in furfural oxidation reactions with hydrogen peroxide in alcohol solutions. No organic acid was used as co-oxidant. Different than other oxidation processes of furfural, the main reactions were obtained without opening of the furan ring [24–26,46]. The impacts of the main reaction variables were assessed. Furfuryl acid and their alkyl esters were selectively obtained.

2. Experimental section

2.1. Chemicals

All the chemicals were acquired from commercial sources and used without previous treatment. All the alcohols were Sigma 99 wt. %. All the metal salts, $FeCl_3{\cdot}6\ H_2O$ (97 wt. %), $AlCl_3{\cdot}6H_2O$ (99.5 wt. %), $CuCl_2{\cdot}2\ H_2O$ (99 wt. %), $CoCl_2{\cdot}6\ H_2O$ (98 wt. %), and $NiCl_2{\cdot}6\ H_2O$ (97 wt. %) were Vetec. Furfural was purchased from Sigma-Aldrich (99 wt. %). $NaHCO_3$ and $Na_2WO_4{\cdot}2\ H_2O$ were Vetec (99 wt. %). $HCl_{(aq)}$ (33 wt. %) was purchased from Dinâmica and Na_2SiO_3 (99 wt. %) was from Sigma-Aldrich. CH_3OH was acquired from Sigma (99 wt. %) Aqueous hydrogen peroxide was purchased from Alphatec (35 wt. %).

2.2. Synthesis of transition metal exchanged Keggin heteropolyacid salts

The syntheses of the transition metal exchanged heteropoly salts were performed through metathesis of the silicotungstic acid with a diluted solution of the metal chlorides as already described the literature [47]. Typically, a solution of $H_4SiW_{12}O_{40}$ (ca. 1 g) was dissolved in water (30 mL) and heated to 333 K with constant magnetic stirring. To this solution was slowly added drop to drop another solution containing metal chloride in stoichiometric amount. The resulting solution was stirred and heating to 333 K/ 3 h. Afterward, the solution was evaporated releasing HCl and giving the solid salt, which was dried at 383 K/ 3 h.

2.3. Characterization of the catalysts

The infrared spectra (FT-IR/ ATR) were recorded on Varian 660-IR spectrometer 660-IR model Fourier transformed infrared coupled to the attenuated total reflectance technique. The patterns of X-rays diffraction (XRD) of the salts were analyzed using a XRD-ray Diffraction System model D8-Discover Bruker using Ni filtered Cu-kα radiation (λ = 1.5418 Å), working at 40 kV and 40 mA, with a counting time 1.0 s in the diffraction angle (2θ) ranging from 5 to 80 degrees.

Crystallite sizes were calculated using the Scherrer equation:

$$L = \frac{K.\lambda}{\beta.\cos\theta} \quad (1)$$

Where λ is the X-ray wavelength in nanometer (nm), β is the peak width of the diffraction peak profile at half maximum height resulting from small crystallite size in radians, and K is a constant related to crystallite shape, normally taken as 0.89.

The porosity properties of the catalysts were evaluated by H_2 adsorption/ desorption isotherms in a NOVA 1200e High Speed, automated surface area and pore size analyzer Quantachrome instrument. Before the analysis, the samples were degassed by 5 h. The surface area was calculated by Brunauer-Emmett-Teller equation applied to the isotherms.

Catalyst acidity was estimated by potentiometric titration, as described in the literature [48]. The electrode potential variation was measured with a potentiometer (i.e. Bel, model W3B). Typically, 50 mg of the salt was dissolved in CH_3CN, magnetically stirred by 3 h and then titrated with *n*-butylamine solution in toluene (ca. 0.025 mol L^{-1}).

The scanning electron microscopy (SEM) images acquired in a JEOL JSM-6010/LA microscope. An energy dispersive spectrometry system (EDS) was used to analyze the chemical composition of catalysts. SEM images and EDS spectra were recorded using 10 mm working distance and 20 KV acceleration voltage. Thermal analyses were carried out in a Perkin Elmer Simultaneous Thermal Analyzer (STA) 6000. Typically, a sample (ca. 10 mg) was heated at a rate of 10 K/ min under N_2 flow. Temperature range of TG curves was 303–973 K.

2.4. Catalytic runs

The catalytic reactions were carried out in a 25 mL three-necked glass flask, fitted with a sampling system and a reflux condenser. Typically, furfural (2.5 mmol) was solved in CH_3OH solution (ca. 10 mL), magnetically stirred and heated to 323 K. After to add the catalyst (ca. 1.0 mol %, 25.0 μmol) and hydrogen peroxide (5.0 mmol), the reaction was started and monitored during 1 h through GC analyses (Shimadzu 2010, FID, Carbowax column) of aliquots periodically collected. The profile of temperature was as follows: 80 °C min^{-1}, 10 °C min^{-1} up to 210 °C, hold time of 13 min. Temperatures of the injector and detector were 250 °C.

Conversion and selectivity were calculated by matching of GC peaks of compounds into respective calibration curves. Dodecane was the internal standard. The main reaction products were identified by mass spectrometry analysis in GC–MS Shimadzu ultra mass spectrometer operating in an electronic impact mode at 70 eV.

The oligomers were quantified through mass balance of reactions, comparing the sum of the GC peak areas of the products with the GC peak area of the furfural consumed (Equation 1).

$$\%\ \text{oligomers} = ((A_0 - A_i) - \Sigma A_p) \times 100 \quad (1)$$

Where:

A_0 = GC peak area of furfural (time = t_0);

A_i = GC peak area of furfural (time = t);

ΣA_p = total sum of GC peak areas of the products after the correction by the response factor, which was determined comparing the GC peak of the pure products with the GC peak of furfural at the same

Table 1
Colors and yielding of the metal exchanged silicotungstic acid salts.

Catalyst	Color	Yielding (%)
$Co_2SiW_{12}O_{40}$	pink	82
$Cu_2SiW_{12}O_{40}$	light blue	88
$Fe_{4/3}SiW_{12}O_{40}$	dark yellow	85
$Ni_2SiW_{12}O_{40}$	light green	91
$Al_{4/3}SiW_{12}O_{40}$	white	96

concentrations.

2.5. Recovery and reuse of the catalyst

After the end of the reaction, the solvent was removed under reduced pressure and 20 mL of water was added. The resulting mixture was three times extracted with ethyl acetate. The aqueous phase was evaporated under heating plate to near dryness and then dried at room conditions. The solid catalyst was weighted and reused in another catalytic run.

3. Results and discussion

3.1. Synthesis and characterization of the catalysts

In general, the solid salt catalysts were synthesized with a high yield (Table 1). No recrystallization procedure was required.

The infrared spectroscopy is a powerful tool to verify if the primary structure of the Keggin HPAs (i.e., heteropolyanion) remained intact after the protons exchange by metal cations. It could be confirmed because the typical absorption bands of the Keggin anion are located at region of $1700-400\,cm^{-1}$. FT-IR/ATR spectra of silicotungstic acid and their transition metal salts were recorded and are presented in Fig. 1.

The main vibration bands of chemical bonds belonging to the silicotungstic anion were observed in the infrared spectra of precursor acid also noticed in the spectra of the transition metal salts. The asymmetric stretching (i.e., ν_{as}) and angular deformation (i.e., δ) of Si-O bonds were observed at 926 and 539 cm^{-1}, respectively. The vibrations of tungsten-oxygen bonds generated bands at following wavenumbers: 980 cm^{-1} ν_{as} (W = O_d), 910 cm^{-1} ν_{as} (W-O_b-W), and 762 cm^{-1} ν_{as} (W-O_c-W). The subscript in the oxygen atoms distinguish them in relation to the place occupied in the heteropolyanion; O_a is the oxygen atom linked to the silicon atom; O_b are those oxygen atoms belonging to the WO_6 octahedral units sharing corners; O_c are the oxygen atoms in edges and O_d are terminal oxygen atoms bonded to the tungsten atoms [49].

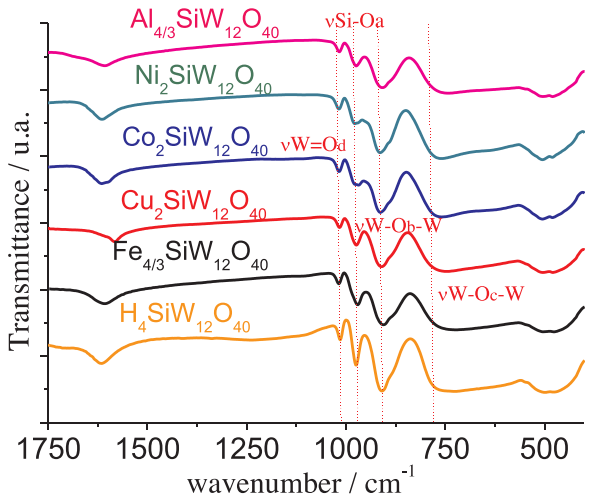

Fig. 1. FT-IR/ ATR spectra of the $H_4SiW_{12}O_{40}$ and their metal exchanged salts.

Fig. 2 shows the XRD patterns of the silicotungstic acid and their metal salts. The main peaks were placed within region 2θ of 5–40 degrees. The parent $H_4SiW_{12}O_{40}$ exhibited all markers of a typical X-ray diffractogram of a body-centered cubic secondary structure of Keggin anion, with characteristic diffraction peaks at angles 9.5, and 26.0 [50]. The profile of the diffractograms obtained from salts of Cu(II), Ni(II), Co (II) and Fe(III) were like the pristine acid. However, different than other salts, Al(III) silicotungstate have no diffraction peaks in the range of $10-20$ 2θ.

The XRD patterns of the Keggin HPAs are related to the secondary structure of these solids, which is affected by the presence of water molecules and H^+ cations; in general, the HPAs have hydrated protons as dihydronium cations (i.e., $H_5O_2^+$), which are coordinated simultaneously to the four terminal oxygen atoms of the heteropolyanions [51]. When the HPAs are converted to metal salts, the presence of these cations may be led to changes in the packaging of the anions and consequently, new lines diffraction or shift of peaks may occur, due to contraction of unit cell [52,53].

Through the Scherrer equation, the crystallite sizes were estimated (Table 1SM). While the silicotungstic acid had crystallite size of 26 nm, the metal salts presented equal or higher values, which ranged from 26 (i.e., $Al_{4/3}SiW_{12}O_{40}$) to 42 nm (i.e., $Fe_{4/3}SiW_{12}O_{40}$). Only the $Cu_2SiW_{12}O_{40}$ salt presented a crystallite size lower than pristine acid (ca. 13.5 nm).

To assess the effect of the protons exchange on the thermal stability of the catalysts, TG/DTG curves of silicotungstic acid and their metal salts were obtained (Fig. 1SM). In the TG/DTG curves of $H_4SiW_{12}O_{40}$ and their salts, the weight at temperatures of 323 K–473 K was assigned to the eliminating of crystallization or physiosorbed water molecules [54]. The total number of water molecules varied from 7 to 12 mol H_2O/ mol catalyst (Table 2SM). At temperatures between 473 and 673 K, the constitutional waters loss giving the $SiW_{12}O_{38}$ oxides and monometallic oxides [55]. The complete decomposition of the heteropolyanion, without a noticeable weight loss occurred at temperatures higher than 773 K [56].

Fig. 3 shows the physical adsorption/desorption isotherms of N_2 and Fig. 3SM the pore diameter distributions of the silicotungstic acid and the metal salts. According to IUPAC recommendations, the isotherms of the synthesized salts can be classified as type as being intermediate between Type III and V. The isotherms of some catalysts (i.e., $H_4SiW_{12}O_{40}$, $Cu_2SiW_{12}O_{40}$ and $Fe_{4/3}SiW_{12}O_{40}$) presented a noticeable type H3 hysteresis loop, which is assigned to the capillarity condensation in mesopores solids due to adsorption on aggregates of platy particles [57].

Table 2 shows the results of the texture parameters of the silicotungstic acid and their metal exchanged salts. The $H_4SiW_{12}O_{40}$ has a very low surface area (ca. 4.1 $m^2\,g^{-1}$), however, the introduction of metal cations slightly increased the surface area from 8.8–10.7 $m^2\,g^{-1}$, excepted in the case of iron salt (ca. 5.1 $m^2\,g^{-1}$). The pore volume of the metal salts was higher than that of the precursor acid (ca. $0.8–1.6 \times 10^{-2}\,m^3\,g^{-1}$ versus $0.6 \times 10^{-2}\,m^3\,g^{-1}$). Nonetheless, the $Ni_2SiW_{12}O_{40}$ salt had the lowest pore volume (ca. $0.6 \times 10^{-2}\,m^3\,g^{-1}$). The pore sizes of metal silicotungstate showing values lower than $H_4SiW_{12}O_{40}$; while the pore diameter of the acid was 3.8 nm, the salts presented pore ranging from $3.1-3.6$ nm, confirming that both acid and salts are mesoporous solids (i.e., mesoporous solids between 2 and 50 nm). These porosity and isothermal adsorption characteristics for heteropoly salts are in accordance to the literature [44,45].

According to the pore diameter distribution curve profiles, the silicotungstic acid and their metal salts presented diameters in the range of mesoporous (Fig. 3SM). Most of the particles presented medium diameter of 3–4 nm, with maximum pore volume of $7 \times 10^{-5}\,cm^3\,nm^{-1}\,g^{-1}$.

The total acidity strength of the silicotungstate catalysts was determined by potentiometric titration using *n*-butylamine (Fig. 4). The

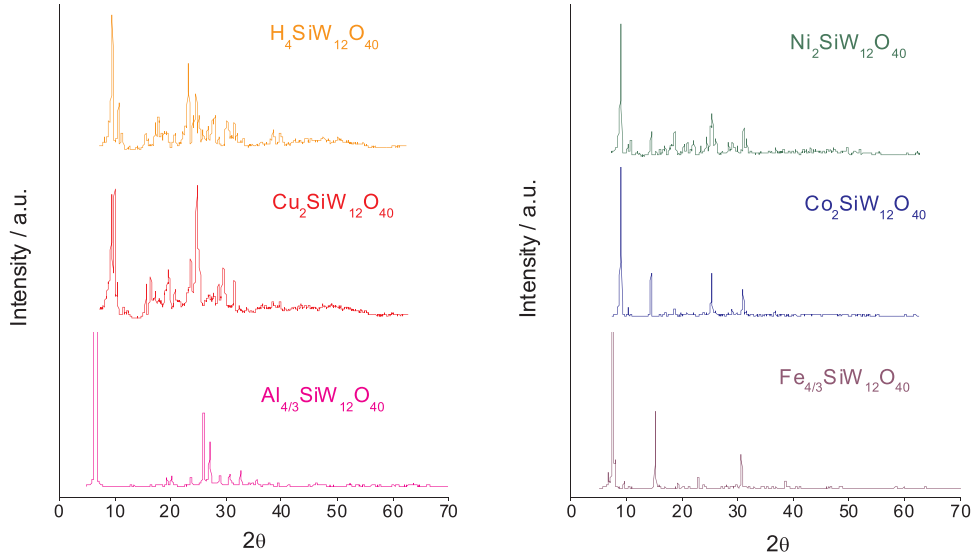

Fig. 2. Powder XRD patterns of the silicotungstic acid and their metal salts.

initial electrode potential (Ei) allows to classify the strength of acid sites as very strong (Ei > 100 mV), strong (0 < Ei < 100 mV), weak Ei < 0 mV) and very weak (Ei < −100 mV) [58]. The acidic sites of all the catalysts were classified as very strong, similarly to the acidic sites of the pristine silicotungstic acid (Fig. 4).

The acidity strength of the metal salts was as follow; $Ni_2SiW_{12}O_{40}$ < $Co_2SiW_{12}O_{40}$ < $Al_{4/3}SiW_{12}O_{40}$ < $Cu_2SiW_{12}O_{40}$ ≅ $Fe_{4/3}SiW_{12}O_{40}$. Although this technique allows determining the total acidity (i.e., Lewis and or Brønsted acid sites), the tendency observed in titration curves of the heteropoly salts obeyed the Lewis acidity of metal cations.

The profile of the titration curves of the metal silicotungstate salts was different than titration curves of silicotungstic acid. In general, lower volumes of *n*-butylamine were required to reach the equivalence point, which are gave by the inflection points observed in the titration curves. The presence of more than one plateau suggests that sites with different strengths are present. The value from which the plateau is attained (meq amine/g salt) indicates the total number of acid sites present in the titrated solid. The number of acidic sites for the silicotungstic acid was 1.35 mEq n-butylamine/ g catalyst. The amount of acid sites presents in the heteropoly salts increase as follows: $Co_2SiW_{12}O_{40}$ < $Ni_2SiW_{12}O_{40}$ < $Al_{4/3}SiW_{12}O_{40}$ ≅ $Cu_2SiW_{12}O_{40}$ < $Fe_{4/3}SiW_{12}O_{40}$.

The sites acid determined by this technique can be Brønsted and/or Lewis type. Analysis of infrared spectroscopy of the metal exchanged HPA salts, adsorbing pyridine or NH_3 demonstrated that they have both types of sites acid [58]. Those authors proposed that, for the neutral salts (i.e., copper and aluminum, silicon(or phospho)tungstate), the Brønsted type acidity is due to the formation of H^+ ions by dissociation of water molecules coordinated to the metallic cation.

In a previous work, we have confirmed the stoichiometric composition of these metal salts by ICP analyses [45]. Herein, the elemental composition of the silicotungstic catalysts was confirmed through EDS analysis (Fig. 3SM). It was found that the elemental composition determined by EDS agree with the theoretical values expected, indicating a successful formation of the metal exchanged heteropoly catalysts. No traces of chloride ions, which were present in the precursor metal salt were detected.

The EDS equipment was coupled to a microscope that provided the MEV images of catalyst surface (Fig. 4SM). The SEM images were obtained a with 2000 x magnifications for the $H_4SiW_{12}O_{40}$ and their metal salts. The SEM images showed that the nickel heteropoly salt presented a lamellar structure with flakes having width of 10–40 microns and the other dimensions around to 100 microns. Regardless of the metal cation, the other salts show a grainy morphology with grains varying from less than 5 microns up to 50 microns. Therefore, we can conclude that the protons exchange by metal cations resulted in a significant alteration on the initial morphology of the silicotungstic acid.

3.2. Catalytic tests

3.2.1. Effect of catalyst nature on the furfural oxidation with hydrogen peroxide in methyl alcohol solutions

Initially, a screening aiming determine the most effective metal salt catalyst was performed using conditions previously described in another oxidation reactions [45]. Although excess of hydrogen peroxide (ca. 1:2), only a poor conversion was achieved in the absence of catalyst (ca. 5 %, Fig. 5).

Regardless of the metal cation, all the reactions in the presence of heteropoly salt catalysts achieved the maximum conversion within the first 20 min of reaction (Fig. 4). Noticeably, the $Cu_2SiW_{12}O_{40}$-catalyzed reaction reached the almost complete conversion at this time, while the other reactions had conversions ranging from 30 to 64 %.

The furfural oxidation reaction may occur with or without rupture of the furan ring. For instance, maleic and or succinic acids have been products commonly obtained in reactions of oxidation over heterogeneous catalysts [18,46]. Conversely, the metal silicotungstate-catalyzed furfural oxidation reaction described herein provided products where the aromatic ring of furfural was preserved (Scheme 1). Furoic acid, methyl furoate ester, 2-furfuraldehyde-dimethyl acetal were the main products identified by GC–MS analyses.

As described in the literature, in metal-catalyzed oxidation reactions with hydrogen peroxide the furfural can be also converted to products with a high molar weight (i.e., oligomers), which are not detectable in gas chromatography analysis. Herein, these products were quantified through the mass balance of reactions, comparing the sum of the GC peak areas of the products with the GC peak area of the furfural consumed (see Equation 1, experimental section). Fig. 6 shows the conversion and the reaction selectivity after 1 h reaction.

When the reactions were carried without a metal silicotungstate catalyst, oligomers and acetal were the preferentially formed product. No oxidation product was detected. We have found that these two competitive reactions, condensation of furfural with methyl alcohol and oligomerization, compromised the selectivity of two goal-products (i.e., furoic acid and methyl furoate). The oligomerization is a very common reaction underwent by the furfural, which involve furan-based

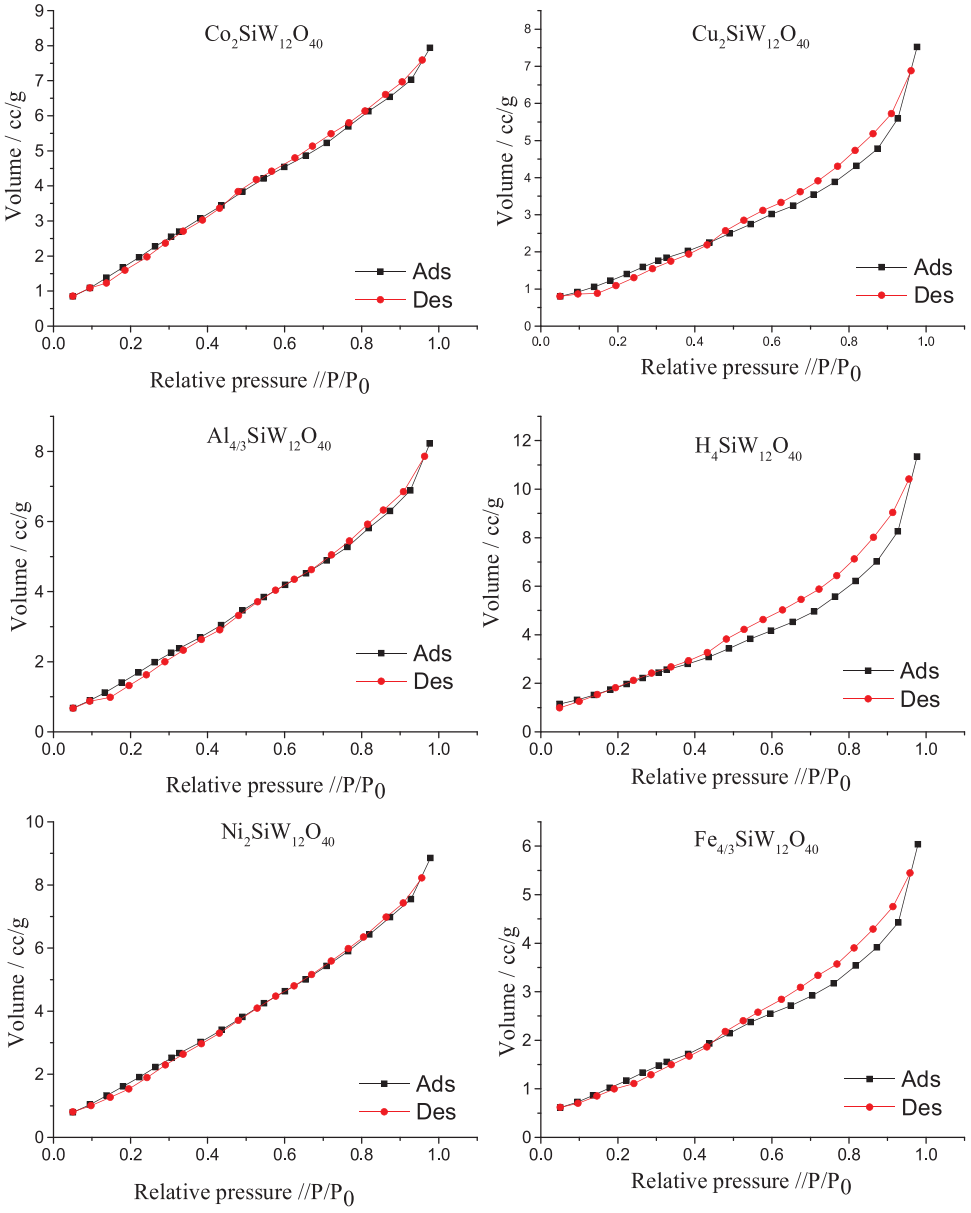

Fig. 3. Isotherms of physical adsorption/desorption of N_2 and pore of the silicotungstic acid and their metal exchanged salts.

Table 2
Surface, volume, and pores size of silicotungstic catalysts.

Entry	Catalyst	Surface area BET[a] ($m^2\ g^{-1}$)	Pores volume (m^3/ g x 10^{-2})	Pores size[b] (nm)
1	$H_4SiW_{12}O_{40}$	4.1	0.6	3.8
2	$Co_2SiW_{12}O_{40}$	9.4	1.1	3.3
3	$Cu_2SiW_{12}O_{40}$	10.7	1.6	3,2
4	$Fe_{4/3}SiW_{12}O_{40}$	5.1	0.8	3.6
5	$Ni_2SiW_{12}O_{40}$	9.5	0.3	3.1
6	$Al_{4/3}SiW_{12}O_{40}$	8.8	1.1	3.2

[a] Multipoint BET method.
[b] DFT method.

intermediates generated during the reaction. This reaction is favored either when peroxide intermediates and or H^+ ions are present [59,60]. Similarly, the condensation furfural with alcohol is also promoted by H^+ ions. These ions can be generated in the hydrolysis involving the water generated in the reaction and the Lewis acid metal cations [58,60].

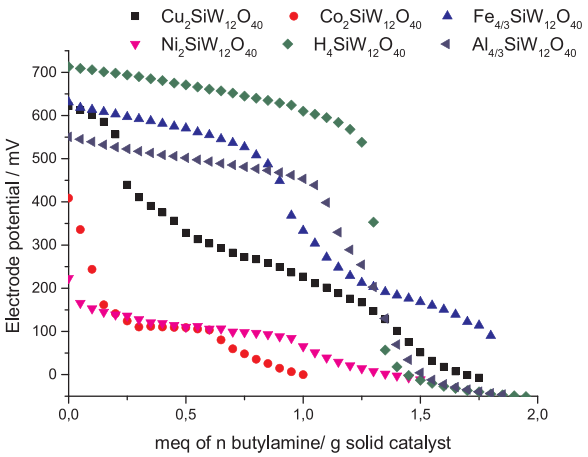

Fig. 4. Potentiometric titration curves with *n*-butylamine of metal exchanged $H_4SiW_{12}O_{40}$ salts.

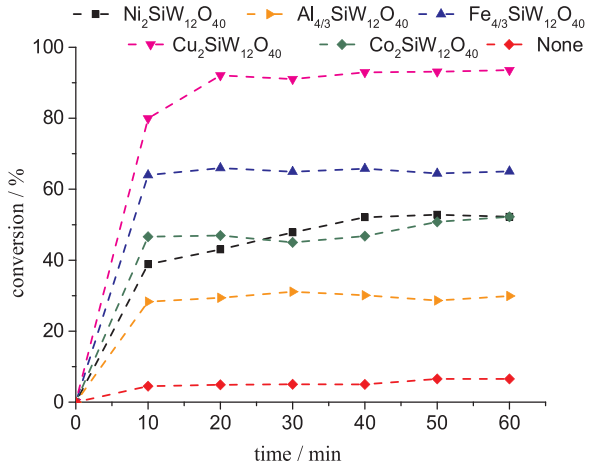

Fig. 5. Effects of catalyst nature on the kinetic curves of furfural oxidation with H_2O_2[a].
[a]Reaction conditions: furfural (2.5 mmol), CH_3OH (9.4 mL, 231 mmol), H_2O_2 (5.0 mmol), temperature (323 K), catalyst (1.0 mol %, 25.0 μmol), volume (10 mL).

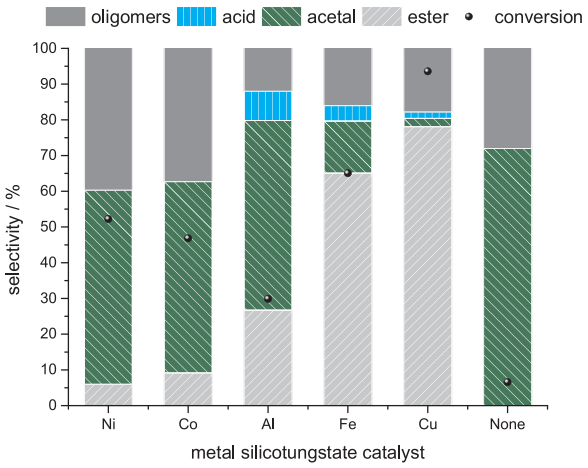

Fig. 6. Conversion and selectivity after 1 h of furfural oxidation with H_2O_2 in the presence of metal silicotungstate catalysts[a].
[a]Reaction conditions: furfural (2.5 mmol), H_2O_2 (5.0 mmol), catalyst (1 mol %, 25 μmol), methyl alcohol (9.4 mL, 231 mmol), temperature (323 K), volume (10.0 mL).

It is noteworthy that the catalysts that were less efficient to oxidize furfural to furoic acid were those most effective to condensate furfural with methyl alcohol; indeed, the higher selectivity toward furfural acetal was achieved in reactions in the presence of $Ni_2SiW_{12}O_{40}$, $Co_2SiW_{12}O_{40}$ or $Al_{4/3}SiW_{12}O_{40}$ catalysts (Fig. 6). Conversely, the reactions that achieved the greater selectivity toward furoate methyl, a product of the oxidative esterification of furfural, were carried out in the presence of the $Fe_{4/3}SiW_{12}O_{40}$ or $Cu_2SiW_{12}O_{40}$ catalyst. The reaction described herein is an attractive alternative to other processes to synthesize alkyl furoates, which involve supported Au nanoparticles catalysts, alkaline conditions, and high pressures of molecular oxygen [27,28,61].

The high efficiency of both metal silicotungstate catalysts (i.e., $Fe_{4/3}SiW_{12}O_{40}$ and $Cu_2SiW_{12}O_{40}$) may be assigned to the highest acidity exhibited by two catalysts (Fig. 4). We suppose that the Lewis and Brønsted acid characters of these catalysts are key aspects in the oxidation and esterification steps, respectively. Moreover, the results showed that in the presence of these catalysts, the furoic acid was almost converted to their ester.

Several works have investigated the nature of acid sites (i.e., Lewis or Brønsted acid sites) using NH_3-TPD measurements [62]. However, in the present case, our catalysts are soluble in methyl alcohol solution, and this technique looks few adequate to the solid catalysts. Nonetheless, it is important to highlight that both acid sites are present in the catalyst structure; while metal cations (i.e., Lewis acid site) react with hydration water or residual in the catalyst anion giving hydrated protons (Brønsted acid sites) [63]. Recently, we performed assessments on the acid sites nature of Sn(II) silicotungstate salt catalysts and confirmed that both types of acid sites remains in heteropoly salts of metal exchanged silicotungstic acid [64].

3.2.2. Effect of load catalyst on the furfural oxidation with hydrogen peroxide in methyl alcohol solutions

Once the $Cu_2SiW_{12}O_{40}$ has demonstrated to be the most efficient catalyst it was selected to assess the effects of the main reaction parameters of esterification oxidative of furfural. To investigate the effect of catalyst load, the reactions were carried at the same previous conditions, varying only the load of $Cu_2SiW_{12}O_{40}$.

An increase in the catalyst load enhanced the reaction conversion only until 1.0 mol %; at higher loads, no beneficial effect was observed. Probably, the high load of the catalyst was more favorable to the oligomerization reactions, consequently diminishing the ester selectivity. Although not shown, this effect was verified using also catalyst load until 1.5 mol %. Another important question is that as the acetalization and esterification reactions are also dependent on catalyst load, mainly of H^+ ions generated in solution, they were also impacted by the variation of catalyst concentration. However, in terms of ester selectivity, 0.75 mol % of catalyst load was the most effective.

3.2.3. Effect of H_2O_2 load on the $Cu_2SiW_{12}O_{40}$-catalyzed furfural oxidation reactions in methyl alcohol

Although the best catalyst load toward oxidative esterification of furfural has been ca. 0.75 mol %, we selected 1.0 mol % to assess the impact of the oxidant on this reaction, aiming make cleaner this effect

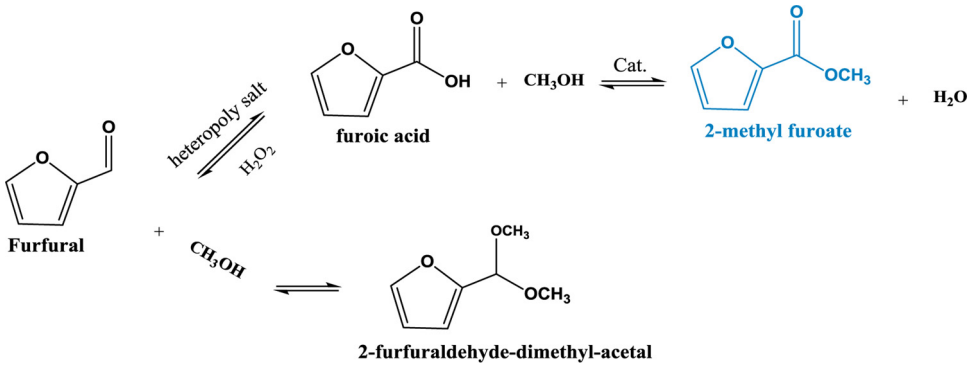

Scheme 1. Main products of metal silicotungstate-catalyzed furfural oxidation with H_2O_2.

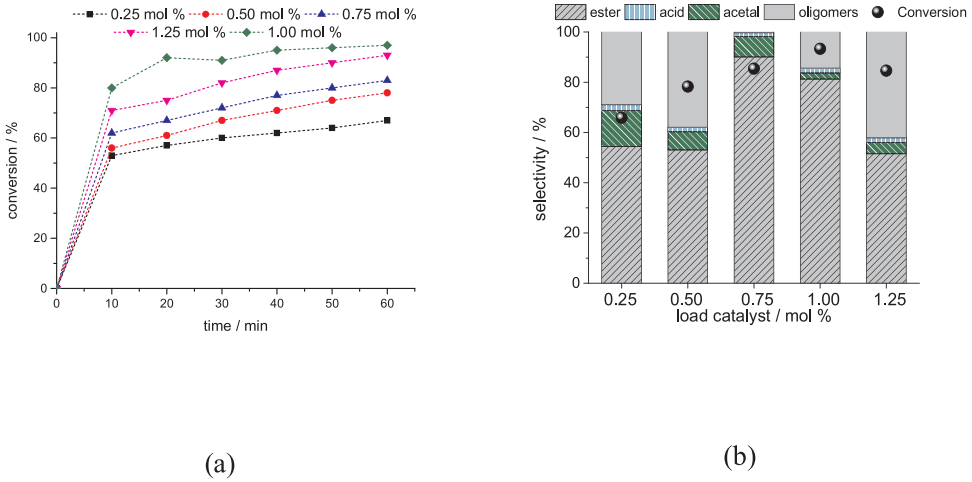

Fig. 7. Effect of catalyst load on the kinetic curves (a), conversion and selectivity (b) of the $Cu_2SiW_{12}O_{40}$-catalyzed furfural oxidation with H_2O_2[a].
[a]Reaction conditions: furfural (2.5 mmol), H_2O_2 (5.0 mmol), methyl alcohol (9.4 mL, 231 mmol), temperature (323 K), volume (10.0 mL).

(Fig. 7).

At a molar ratio of furfural: oxidant higher than 1:2, no significant effect was observed in the reaction conversion, like the observed in products selectivity (Fig. 8a and b, respectively). The usage of an equimolar amount of oxidant reduced either the furfural conversion as well as the ester selectivity. Expectedly, a lower load of oxidant compromised the oxidation reaction and consequently the furfural acetalization was more favored.

Fig. 9 describes the shows that at the reaction conditions, a part of hydrogen peroxide is decomposed even in the absence of furfural or catalyst (Fig. 9b). Conversely, furfural was minimally converted when oxidant and catalyst were absent (Fig. 9a). When catalysts such as palladium salts are used in oxidation reactions with hydrogen peroxide, the oxidant is quickly decomposed, mainly in the absence of substrate [64]. However, in this case, there was only a small increase in consumption of peroxide when the copper silicotungstate was present.

3.2.4. Impacts of temperature on the $Cu_2SiW_{12}O_{40}$-catalyzed furfural oxidation reactions in methyl alcohol

The literature has described that furfural acetalization with methyl alcohol in the presence of Lewis or Bronsted acid catalysts proceed efficiently at room temperature [58,59]. Thus, we decided to verify if the oxidation reaction of furfural could have a similar behavior.

Table 3 summarize the main results.

An increase of temperature favored the furfural oxidation to furoic acid, which was almost completely converted to methyl furoate. At low temperatures, the oxidation was compromised and consequently the acetalization of furfural was enhanced. Although no shown herein, the kinetic and the selectivity of reaction was monitored collecting aliquots at regular time intervals (ca. 10 min). Regardless of reaction temperature, all the reactions achieved the maximum conversion within the first 30 min of reaction. No changes in the reaction selectivity where noticed after this period.

3.2.5. $Cu_2SiW_{12}O_{40}$-catalyzed furfural oxidation reactions with hydrogen peroxide in alkyl alcohol solutions and in acetonitrile solution

The steric hindrance on the hydroxyl group of the alcohol as well as the size of carbon chain are aspects that may affect their reactivity in esterification reactions. To investigate this effect, the oxidative esterification of furfural was also investigated in solutions of different alkyl alcohols (Fig. 10).

In terms of conversion, the probable effects were verified; the reactivity of the alcohols was dependent of carbon chain size (i.e., methyl > ethyl > propyl > butyl alcohols) and isopropyl alcohol, a secondary alcohol was the less reactive. Conversely, the selectivity of products led to conclusion that when alcohols with lengthier carbon chains higher than methyl alcohol are present, there was a decrease in the selectivity of esters, and consequently the selectivity of furoic acid increase. The same effect occurred when isopropyl alcohol was the substrate.

The oxidation of the furfural was carried also in acetonitrile solutions at the same reaction conditions used in Fig. 10. No conversion happened in the absence of catalyst. Conversely, a poor conversion was achieved in the presence of the $Cu_2SiW_{12}O_{40}$ catalyst (ca. 14 %). Furoic

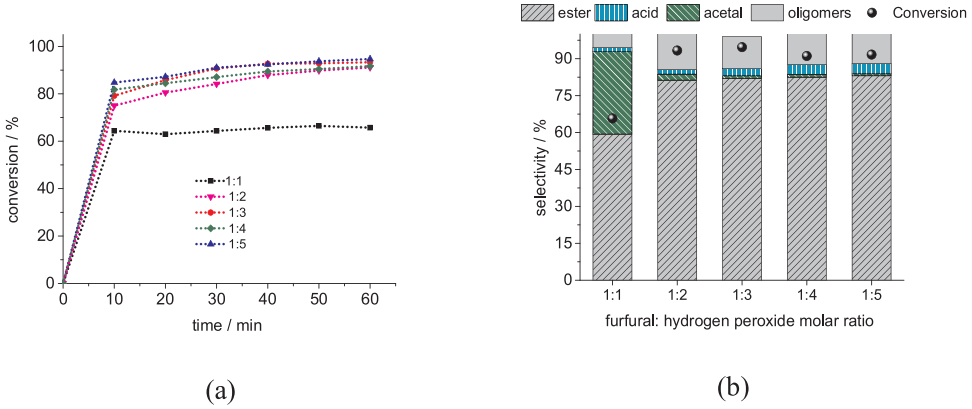

Fig. 8. Effect of oxidant load on the kinetic curves (a), conversion and selectivity (b) of the $Cu_2SiW_{12}O_{40}$-catalyzed furfural oxidation with H_2O_2[a].
[a]Reaction conditions: furfural (2.5 mmol), $Cu_2SiW_{12}O_{40}$ (1.0 mol %), methyl alcohol (9.4 mL, 231 mmol), temperature (323 K), volume (10.0 mL).

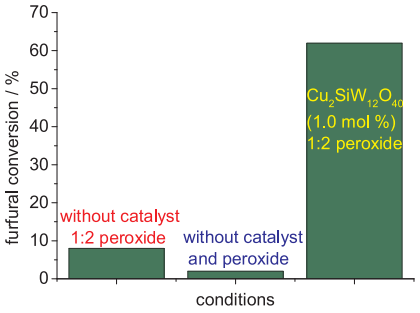

(a)

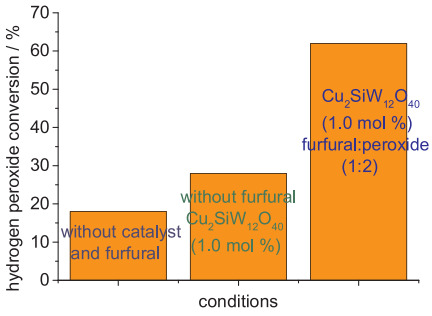

(b)

Fig. 9. Effect of composition of system on the conversion of furfural (a) and hydrogen peroxide (b) in the presence or absence of $Cu_2SiW_{12}O_{40}$ catalyst[a,b].
[a]Reaction conditions: furfural (2.5 mmol), $Cu_2SiW_{12}O_{40}$ (1.0 mol %), methyl alcohol (9.4 mL, 231 mmol), temperature (323 K), volume (10.0 mL).
[b]Reaction conversions were determined by GC analysis (i.e., furfural conversion), and $KMnO_4$ titration (i.e., hydrogen peroxide conversion).

acid was the only product detected. It is possible that as described in other oxidation reactions with tungsten catalysts, a protic solvent may favor the oxidation process stabilizing key reaction intermediates [65].

3.2.6. Reuse and recycle of $Cu_2SiW_{12}O_{40}$ catalyst in furfural oxidation reactions in methyl alcohol with hydrogen peroxide

The $Cu_2SiW_{12}O_{40}$ catalyst was reused as described in Section 2.5, which was previously optimized in previous works with furfural and methyl alcohol [59,60] (Fig. 11).

After the solvent removal, water and ethyl acetate were added to the remaining neat; after has been washed three times, the aqueous phase was dried giving the solid catalyst. Fig. 10 summarizes the main results. High recovery rates of the catalyst were obtained, demonstrating the efficiency of recycling procedure. No significant decreasing in the conversion of furfural was noticed after the successive cycles of reuse. Although omitted in Fig. 10, the reaction selectivity was maintained constant while the catalyst was reused.

Besides the recyclability, the copper silicotungstate catalyst has another relevant advantage; a comparison of TOF measured in the oxidation of furfural with hydrogen peroxide in the presence of different metal silicotungstate salts showed that $Cu_2SiW_{12}O_{40}$ salt is a highly active catalyst (Table 3SM).

Finally, we would like to highlight that a total understanding of the catalytic activity of metal silicotungstate salt certainly per pass by an investigation about how the introduction metal cations affect the redox potential of silicotungstic anion. Nonetheless, it requires theoretical and experimental studies, such as those performed by Zhang et al., which recently assessed the impacts of Pd, Pt or Rh single atoms on the activity of Keggin heteropolyacids in oxidation reactions [61,66,67]. However, this sort of investigation requires gas phase reactions, with model molecules, where the powerful spectroscopy techniques can provide insights on the catalyst structure and their interaction with reactants in situ.

4. Conclusion

In this work, a series of metal exchanged silicotungstic acid salts were easily synthesized and evaluated in oxidative esterification reactions of the furfural with methyl alcohol using hydrogen peroxide as the oxidant. Among the metal silicotungstate salts tested, the $Cu_2SiW_{12}O_{40}$ was the most active and selective toward methyl furoate, the goal product. Different than various processes described in the literature, in this route the furfural was selectively oxidized by aqueous H_2O_2 and converted to ester without opening the furan ring; furoic acid, alkyl furoate and 2-furfural dimethyl acetal were the products formed. Parameters such as the H_2O_2: furfural molar ratio, the catalyst amount, and the temperature have been studied. The reactivity of the furfural with other alkyl alcohols was also assessed. The high conversion and ester selectivity, the mild reaction conditions, the short reaction time, the use of an inexpensive, liquid, non-flammable, and an environmentally benign oxidant, besides a solid, easily synthesizable, and recyclable catalyst, are positive aspects of this process.

Credit author statement

Marcio Jose da Silva, state that all authors (Marcio Jose da Silva and Alana Alves Rodrigues made substantial contributions to all of the following:

(1) the conception and design of the study, acquisition of data, analysis and interpretation of data, (2) drafting the article or revising it critically for important intellectual content, (3) final approval of the version to be submitted.

Declaration of Competing Interest

The authors declare that they have no known competing financial interests or personal relationships that could have appeared to influence the work reported in this paper.

Table 3
Effect of temperature on the conversion and selectivity of the $Cu_2SiW_{12}O_{40}$-catalyzed furfural oxidation with H_2O_2[a].

Exp.	Temperature (K)	Conversion (%)	Selectivity (%)			
			Methyl furoate	Furoic acid	Furfural Acetal	Oligomers
1	298	70	50	0	20	30
2	308	78	57	1	16	26
3	318	89	68	2	11	19
4	328	98	79	2	4	15

[a] Reaction conditions: furfural (2.5 mmol), $Cu_2SiW_{12}O_{40}$ (1.0 mol %), methyl alcohol (9.4 mL, 231 mmol), H_2O_2 (5.0 mmol), volume (10.0 mL).

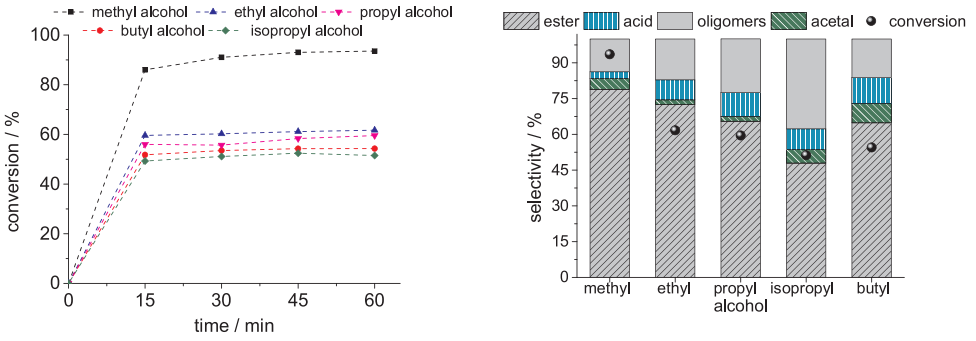

(a) (b)

Fig. 10. $Cu_2SiW_{12}O_{40}$-catalyzed furfural oxidation reactions with hydrogen peroxide in alkyl alcohols solutions[a].
[a]Reaction conditions: furfural (2.5 mmol), $Cu_2SiW_{12}O_{40}$ (1.0 mol %), alkyl alcohol (9.4 mL), H_2O_2 (5.0 mmol), volume (10.0 mL).

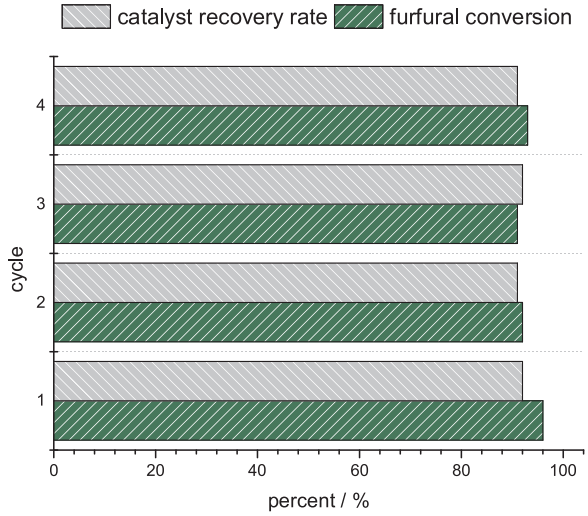

Fig. 11. Reuse and recycle of $Cu_2SiW_{12}O_{40}$ catalyst in oxidations of furfural with H_2O_2 in CH_3OH solutions[a].
[a]Reaction conditions: furfural (2.5 mmol), $Cu_2SiW_{12}O_{40}$ (1.0 mol %), CH_3OH (9.5 mL), H_2O_2 (5.0 mmol), volume (10.0 mL).

Acknowledgements

This study was financed in part by the Coordenação de Aperfeiçoamento de Pessoal de Nível Superior - Brasil (CAPES) - Finance Code 001.

The authors are grateful for the financial support from CNPq and FAPEMIG (Brazil).

Appendix A. Supplementary data

Supplementary material related to this article can be found, in the online version, at doi:https://doi.org/10.1016/j.mcat.2020.111104.

References

[1] R. Mariscal, P. Maireles-Torres, M. Ojeda, I. Sádaba, M. López Granados, Furfural: a renewable and versatile platform molecule for the synthesis of chemicals and fuels, Synth. Lect. Energy Environ. Technol. Sci. Soc. 9 (2016) 1144–1189.
[2] C.M. Cai, T. Zhang, R. Kumar, C.E. Wyman, Integrated furfural production as a renewable fuel and chemical platform from lignocellulosic biomass, J. Chem. Technol. Biotechnol. 89 (2014) 2–10.
[3] P. Gallezot, Conversion of biomass to selected chemical products, Chem. Soc. Rev. 41 (2012) 1538–1558.
[4] N. Alonso-Fagúndez, M. Ojeda, R. Mariscal, J.L.G. Fierro, M. López Granados, Gas phase oxidation of furfural to maleic anhydride on V2O5 /γ-Al_2O_3 catalysts: reaction conditions to slow down the deactivation, J. Catal. 348 (2017) 265–275.
[5] X. Li, B. Ho, D.S.W. Lim, Y. Zhang, Highly efficient formic acid-mediated oxidation of renewable furfural to maleic acid with H_2O_2, Green Chem. 19 (2017) 914–918.
[6] R. Ciriminna, L. Albanese, F. Meneguzzo, M. Pagliaro, Hydrogen peroxide: a key chemical for today's sustainable development, ChemSusChem. 9 (2016) 3374–3381.
[7] A. Bohre, S. Dutta, B. Saha, M.M. Abu-Omar, Upgrading furfurals to drop-in biofuels: an overview, ACS Sustain. Chem. Eng. 3 (2015) 1263–1277.
[8] H. Choudhary, S. Nishimura, K. Ebitani, Highly efficient aqueous oxidation of furfural to succinic acid using reusable heterogeneous acid catalyst with hydrogen peroxide, Chem. Lett. 41 (2012) 409–411.
[9] K.J. Zeitsch, The Chemistry and Technology of Furfural and Its Many By-products, Elsevier, 2000.
[10] A. Amarasekara, N. Okorie, 1-(Alkylsulfonic)-3-methylimidazolium chloride Bronsted acidic ionic liquid catalyzed hydrogen peroxide oxidations of biomass derived furan aldehydes, Catal. Commun. 108 (2018) 108–112.
[11] X. Li, X. Lan, T. Wang, Selective oxidation of furfural in a bi-phasic system with homogeneous acid catalyst, Catal. Today 276 (2016) 97–104.
[12] H. Guo, G. Yin, Catalytic aerobic oxidation of renewable furfural with phosphomolybdic acid catalyst: an alternative route to maleic acid, Phys. Chem. C. 115 (2011) 17516–17522.
[13] I.N.C. Kiran, K. Lalwani, A. Sudalai, N-Heterocyclic carbene catalyzed esterification of aromatic aldehydes with alcohols under aerobic conditions, RSC Adv. 3 (2013) 1695–1698.
[14] M. Manzoli, F. Menegazzo, M. Signoretto, D. Marchese, Biomass derived chemicals: furfural oxidative esterification to methyl-2-furoate over gold catalysts, Catalysts. 6 (2016) 107–134.
[15] H. Cui, X. Tong, L. Yu, M. Zhang, Y. Yan, X. Zhuang, A catalytic oxidative valorization of biomass-derived furfural with ethanol by copper/azodicarboxylate system, Catal. Today 319 (2019) 100–104.
[16] X. Tong, Z. Zhang, Y. Gao, Y. Zhang, L. Yu, Y. Li, Selective carbon-chain increasing of renewable furfural utilizing oxidative condensation reaction catalyzed by monodispersed palladium oxide, Mol. Catal. 477 (2019) 1–8.
[17] X. Li, Y. Zhang, The conversion of 5-hydroxymethyl furfural (HMF) to maleic anhydride with vanadium-based heterogeneous catalysts, Green Chem. 18 (2015) 643–647.
[18] X. Li, B. Ho, Y. Zhang, Selective aerobic oxidation of furfural to maleic anhydride with heterogeneous Mo–V–O catalysts, Green Chem. (2016) 2976–2980.
[19] O. Casanova, S. Iborra, A. Corma, Biomass into chemicals: one pot-base free oxidative esterification of 5-hydroxymethyl-2-furfural into 2,5-dimethylfuroate with gold on nanoparticulated ceria, J. Catal. 265 (2009) 109–116.
[20] S. Kegnæs, J. Mielby, U.V. Mentzel, T. Jensen, P. Fristrup, A. Riisager, One-pot synthesis of amides by aerobic oxidative coupling of alcohols or aldehydes with amines using supported gold and base as catalysts, Chem. Commun. (Camb.) 48 (2012) 2427–2429.
[21] F. Pinna, A. Olivo, V. Trevisan, F. Menegazzo, M. Signoretto, M. Manzoli, F. Boccuzzi, The effects of gold nanosize for the exploitation of furfural by selective oxidation, Catal. Today 203 (2013) 196–201.
[22] B. Martin, J. Sedelmeier, A. Bouisseau, P. Fernandez-Rodriguez, J. Haber, F. Kleinbeck, S. Kamptmann, F. Susanne, P. Hoehn, M. Lanz, L. Pellegatti, F. Venturoni, J. Robertson, M.C. Willis, B. Schenkel, Toolbox study for application of hydrogen peroxide as a versatile, safe and industrially-relevant green oxidant in continuous flow mode, Green Chem. (2017) 1439–1448.
[23] N. Alonso-Fagundez, I. Agirrezabal-Telleria, P.L. Arias, J.L.G. Fierro, R. Mariscal, M.L. Granados, Aqueous-phase catalytic oxidation of furfural with H_2O_2: high yield of maleic acid by using titanium silicalite-1, RSC Adv. 4 (2014) 54960–54972.
[24] A.C. Alba-Rubio, J.L.G. Fierro, L. León-Reina, R. Mariscal, J.A. Dumesic, M. López

Granados, Oxidation of furfural in aqueous H_2O_2 catalysed by titanium silicalite: deactivation processes and role of extraframework Ti oxides, Appl. Catal. B Environ. 202 (2017) 269–280.
[25] Y. Lou, S. Marinkovic, B. Estrine, W. Qiang, G. Enderlin, Oxidation of furfural and furan derivatives to maleic acid in the presence of a simple catalyst system based on acetic acid and TS-1 and hydrogen peroxide, ACS Omega 5 (2020) 2561–2568.
[26] R. Wojcieszak, F. Santarelli, S. Paul, F. Dumeignil, F. Cavani, R.V. Gonçalves, Recent developments in maleic acid synthesis from bio-based chemicals, Sustain. Chem. Process. (2015) 9–20.
[27] F. Menegazzo, M. Signoretto, F. Pinna, M. Manzoli, V. Aina, G. Cerrato, F. Boccuzzi, Oxidative esterification of renewable furfural on gold-based catalysts: Which is the best support? J. Catal. 309 (2014) 241–247.
[28] X.L. Tong, Z.H. Liu, L.H. Yu, Y.D. Li, A tunable process: catalytic transformation of renewable furfural with aliphatic alcohols in the presence of molecular oxygen, Chem. Commun. (Camb.) 51 (2015) 3674–3677.
[29] Z. Liu, X. Tong, J. Liu, S. Xue, A smart catalyst system for the valorization of renewable furfural in aliphatic alcohols, Catal. Sci. Technol. 6 (2016) 1214–1221.
[30] S.-S. Wang, G.-Y. Yang, Recent advances in polyoxometalate-catalyzed reactions, Chem. Rev. 115 (2015) 4893–4962.
[31] M.J. Da Silva, N.A. Liberto, Soluble and solid supported Keggin heteropolyacids as catalysts in reactions for biodiesel production: challenges and recent advances, Curr. Org. Chem. (2016) 1263–1283.
[32] J. Lan, J. Lin, Z. Chen, G. Yin, Transformation of 5- hydroxymethylfurfural (HMF) to maleic anhydride by aerobic oxidation with heteropolyacid catalysts, ACS Catal. 5 (2015) 2035–2041.
[33] N.C. Coronel, M.J. da Silva, Lacunar Keggin heteropolyacid salts: soluble, solid and solid-supported catalysts, J. Clust. Sci. 29 (2018) 195–205.
[34] D.C. Batalha, S.O. Ferreira, R.C. da Silva, M.J. da Silva, Cesium-exchanged lacunar Keggin heteropolyacid salts: efficient solid catalysts for the green oxidation of terpenic alcohols with hydrogen peroxide, Chem. Sel. (2020) 1976–1986.
[35] M.J. da Silva, P.H. da S. Andrade, S.O. Ferreira, C.B. Vilanculo, C.M. Oliveira, Monolacunary $K_8SiW_{11}O_{39}$-catalyzed terpenic alcohols oxidation with hydrogen peroxide, Catal. Letters 148 (2018) 2516–2527.
[36] C.B. Vilanculo, M.J. da Silva, Unraveling the role of the lacunar $Na_7PW_{11}O_{39}$ catalyst in the oxidation of terpene alcohols with hydrogen peroxide at room temperature, New J. Chem. (2020) 2813–2820.
[37] C.B. Vilanculo, M.J. da Silva, M.G. Teixeira, J.A. Villarreal, One-pot synthesis at room temperature of epoxides and linalool derivative pyrans in monolacunary $Na_7PW_{11}O_{39}$-catalyzed oxidation reactions by hydrogen peroxide, RSC Adv. 10 (2020) 7691–7697.
[38] C.B. Vilanculo, M.J. da Silva, S.O. Ferreira, M.G. Teixeira, A rare oxidation of camphene to acid and aldehyde in the presence of Lacunar Keggin heteropoly salts, Mol. Catal. 478 (2019) 110589–110596.
[39] M.J. da Silva, C.M. de Oliveira, Catalysis by Keggin heteropolyacid salts, Curr. Catal. 7 (2018) 26–34.
[40] M.J. da Silva, C.B. Vilanculo, M.G. Teixeira, A.A. Júlio, Catalysis of vegetable oil transesterification by Sn (II)-exchanged Keggin heteropolyacids: bifunctional solid acid catalysts, React. Kinet. Mech. Catal. 122 (2017) 1011–1030.
[41] P.F. Pinheiro, D.M. Chaves, M.J. da Silva, One-pot synthesis of alkyl levulinates from biomass derivative carbohydrates in tin(II) exchanged silicotungstates-catalyzed reactions, Cellulose 26 (2019) 7953–7969.
[42] M.J. da Silva, A.A. Julio, S.O. Ferreira, R.C. Da Silva, D.M. Chaves, Tin(II) phosphotungstate heteropoly salt: an efficient solid catalyst to synthesize bioadditives ethers from glycerol, Fuel 254 (2019) 115607–115618.
[43] D.M. Chaves, S.O. Ferreira, R.C. da Silva, R. Natalino, M.J. da Silva, Glycerol esterification over Sn(II)-exchanged Keggin heteropoly salt catalysts: effect of thermal treatment temperature, Fuel 33 (2019) 7705–7716.
[44] M.J. da Silva, N.A. Liberto, L.C.A. Leles, U.A. Pereira, $Fe_4(SiW_{12}O_{40})_3$-catalyzed glycerol acetylation: synthesis of bioadditives by using highly active Lewis acid catalyst, J. Mol. Catal. A Chem. 422 (2016) 69–83.
[45] M.J. da Silva, L.C. de A. Leles, S.O. Ferreira, R.C. da Silva, K. de V. Viveiros, D.M. Chaves, P.F. Pinheiro, A rare carbon skeletal oxidative rearrangement of camphene catalyzed by Al-exchanged Keggin heteropolyacid salts, Chem. Sel. 4 (2019) 7665–7672.
[46] H. Choudhary, S. Nishimura, K. Ebitani, Metal-free oxidative synthesis of succinic acid from biomass-derived furan compounds using a solid acid catalyst with hydrogen peroxide, Appl. Catal. A Gen. 458 (2013) 55–62.
[47] C. Rocchiccioli-Deltcheff, M. Fournier, R. Franck, R. Thouvenot, Vibrational investigations of polyoxometalates. 2. Evidence for anion-anion interactions in molybdenum(VI) and tungsten(VI) compounds related to the Keggin structure, Inorg. Chem. 22 (1983) 207–216.
[48] L. Méndez, R. Torviso, L. Pizzio, M. Blanco, 2-Methoxynaphthalene acylation using aluminum or copper salts of tungstophosphoric and tungstosilicic acids as catalysts, Catal. Today 173 (2011) 32–37.
[49] A. Popa, V. Sasca, D. Bajuk–Bogdanovi, I. Holclajtner–Antunovic, Synthesis, characterization and thermal stability of cobalt salts of Keggin-type heteropolyacids supported on mesoporous silica, J. Therm. Anal. Calorim. 126 (2016) 1567–1577.
[50] F.J. Berry, G.R. Derrick, M. Mortimer, Identification and characterisation of stable phases of silicotungstic acid, $H_4SiW_{12}O_{40}{\cdot}nH_2O$, Polyhedron 68 (2014) 17–22.
[51] P. Villabrille, G. Romanelli, L. Gassa, P. Vazquez, C. Caceres, Synthesis and characterization of Fe-and Cu-doped molybdovanadophosphoric acids and their application in catalytic oxidation, Appl. Catal. A Gen. 324 (2007) 69–76.
[52] S. Borghese, B. Louis, A. Blanc, P. Pale, Design of silver (I)-heteropolyacids: toward the molecular control of reactivity in organic chemistry, Catal. Sci. Technol. 1 (2011) 981–986.
[53] I.V. Kozhevnikov, Heterogeneous acid catalysis by heteropoly acids: approaches to catalyst deactivation, J. Mol. Catal. A Chem. 305 (2009) 104–111.
[54] L.R. Pizzio, M.N. Blanco, A contribution for the physicochemical characterization of nonstoichiometric salts of silicotungstic acid, Microporous Mesoporous Mater. 103 (2007) 40–47.
[55] R.M. Ladera, J.L.G. Fierro, M. Ojeda, S. Rojas, Keggin heteropolyacids supported on TiO_2 used in gas-solid (photo)catalytic propene hydration and in liquid-solid photocatalytic glycerol dehydration, J. Catal. 312 (2014) 195–203.
[56] K.S.W. Sing, D.H. Everett, R.A.W. Haul, L. Moscou, R.A. Pieroti, J. Rouquerol, T. Siemieniewska, Reporting physisorption data for gas/solid systems with special reference to the determination of surface area and porosity, Pure Appl. Chem. 57 (4) (1985) 603–619.
[57] L. Méndez, R. Torviso, L.R. Pizzio, M.N. Blanco, 2-Methoxynaphthalene acylation using aluminum or copper salts of tungstophosphoric and tungstosilicic acids as catalysts, Catal. Today 173 (1) (2011) 32–37.
[58] V.M. Fuchs, L.R. Pizzio, Mirta N. Blanco, Hybrid materials based on aluminum tungstophosphate or tungstosilicate as catalysts in anisole acylation, Catal. Today 133–135 (2008) 181–186.
[59] M.G. Teixeira, R. Natalino, M.J. da Silva, A kinetic study of heteropolyacid-catalyzed furfural acetalization with methanol at room temperature via ultraviolet spectroscopy, Catal. Today 344 (2018) 143–149.
[60] M.J. da Silva, M.G. Teixeira, Assessment on the double role of the transition metal salts on the acetalization of furfural: lewis and Brønsted acid catalysts, Mol. Catal. 461 (2018) 40–47.
[61] M. Douthwaite, X. Huang, S. Iqbal, P.J. Miedziak, G.L. Brett, S.A. Kondrat, J.K. Edwards, M. Sankar, D.W. Knight, D. Bethell, G.J. Hutchings, The controlled catalytic oxidation of furfural to furoic acid using AuPd/$Mg(OH)_2$, Catal. Science Technol 7 (2017) 5284–5293.
[62] B. Zhang, G. Sun, S. Ding, H. Asakura, J. Zhang, P. Sautet, N. Yan, Atomically dispersed Pt_1–polyoxometalate catalysts: how does metal–support interaction affect stability and hydrogenation activity? J. Am. Chem. Soc. 141 (20) (2019) 8185–8197.
[63] M.J. da Silva, A.A. Rodrigues, P.F. Pinheiro, Solketal synthesis from glycerol and acetone in the presence of metal salts: A Lewis or Brønsted acid catalyzed reaction? Fuel 276 (2020) 188164 -118172.
[64] M.J. da Silva, D.M. Chaves, A.A. Julio, F.A. Rodrigues, C.G.O. Bruziquesi, Sn(II)-exchanged Keggin silicotungstic acid-catalyzed etherification of glycerol and ethylene glycol with alkyl alcohols, Ind. Eng. Chem. Res. 59 (21) (2020) 9858–9868.
[65] A.A. de Oliveira, M.L. da Silva, M.J. da Silva, Palladium-catalysed oxidation of bicycle monoterpenes by hydrogen peroxide in acetonitrile solutions: a metal re-oxidant-free and environmentally benign oxidative process, Catal Lett 130 (2009) 424–431.
[66] L.A.S. Viana, G.R.N. da Silva, M.J. da Silva, A highly selective Na_2WO_4-catalyzed oxidation of terpenic alcohols by hydrogen peroxide, Catal. Let. 148 (2018) 374–382.
[67] M.J. Hülsey, B. Zhang, Z. Ma, H. Asakura, D.A. Do, W. Chen, T. Tanaka, P. Zhang, Z. Wu, N. Yan, In situ spectroscopy-guided engineering of rhodium single-atom catalysts for CO oxidation, Nat. Commun. 10 (2019) 1330–1340.